Full Paper

Physicochemical Properties and Photodynamic Activity of Novel Derivatives of Triarylmethane and Thiazine

María N. Montes de Oca[1]*, Jimena Vara[1]*, Laura Milla[2], Viviana Rivarola[2], and Cristina S. Ortiz[1]

[1] Facultad de Ciencias Químicas, Departamento de Farmacia, Universidad Nacional de Córdoba, Ciudad Universitaria, Córdoba, Argentina
[2] Facultad de Ciencias Exactas, Departamento de Biología Molecular, Físico-químicas y Naturales, Universidad Nacional de Río Cuarto, Córdoba, Argentina

Triarylmethane and thiazine dyes have attracted attention as anticancer and antimicrobial agents, due to their structural features and selective localizations. Although these dyes have been initially explored in the context of photodynamic therapy, some of these such as New Fuchsin and Azure B have still not been extensively investigated. For this reason, we evaluated the chemical stability, aggregation effect, and lipophilicity, as well as the photodynamic activity against LM-2 murine mammary carcinoma cells of five new brominated dyes of triarylmethane and thiazine. These cationic compounds were obtained at high purities and unequivocally characterized by conventional techniques. The introduction of bromine atoms into the chromophoric system of New Fuchsin and Azure B dyes gave rise to a moderate bathochromic shift and increased the lipophilicity, thereby improving their photophysical and photochemical properties for biomedical applications. Moreover, the *in vitro* photodynamic activity demonstrated that, as the degree of bromination increased, the phototoxicity remained unchanged or decreased. The lower efficiency to inactivate cultured tumor cells may be attributed to the formation of the colorless carbinol pseudobase and aggregation effects for triarylmethane and thiazine dyes, respectively. A promising strategy to reverse the biological activity decrease observed might be the design of third-generation photosensitizers.

Keywords: Azure B / Bromination / New Fuchsin / Photodynamic activity / Physicochemical properties

Received: November 19, 2012; Revised: January 3, 2013; Accepted: January 18, 2013

DOI 10.1002/ardp.201200437

Additional supporting information may be found in the online version of this article at the publisher's web-site

Introduction

Photodynamic therapy (PDT) treatment consists in first loading the target cells with a photosensitizer. Then, upon irradiation with light of an appropriate frequency, the energy of the activated photosensitizer is subsequently transferred to molecular oxygen to produce singlet oxygen and other reactive oxygen species that cause cell death [1–3]. The current and potential uses of dyes as photosensitizers have led to further detailed studies on their chemical properties and impact on the bioenvironment. Cationic dyes have a major capability to accumulate in mitochondria of tumor cells due to their negative membrane potential being higher than that of the normal cells, a characteristic that improves their application in this therapy [4–7].

The effectiveness of PDT treatment depends on the physiological and physicochemical properties of the photosensitizer. Second-generation photosensitizers have been developed to improve properties such as chemical purity, composition, cytotoxicity only in the presence of light, preferential retention by the target tissue, photochemical reactivity, the effective production of singlet oxygen and other reactive oxygen species, and a high extinction coefficient with a strong absorbance at longer wavelengths (550–800 nm) [1–3]. One strategy used to

Correspondence: Dr. Cristina S. Ortiz, Facultad de Ciencias Químicas, Ciudad Universitaria, Universidad Nacional de Córdoba, madina Allende esq. Haya de la Torre, Córdoba X5000HUA, Argentina.
E-mail: crisar@fcq.unc.edu.ar
Fax: +54 351 5353865 int. 53364

*These authors contributed equally to this article.

improve the therapeutic capability of the photosensitizers is through the heavy atom effect. This substitution increases the production of the singlet oxygen by enhancing the intersystem crossing and producing a red shift of the maximum absorption wavelength [3, 8, 9]. Consequently, an appropriate choice of drug type and dose, light wavelength, and drug-light interval can improve the efficacy and safety of PDT.

Thiazine and triarylmethane dyes can accumulate preferentially in the mitochondria of malignant cells and possess phototoxic effects [4, 10, 11]. For example, Methylene Blue has been demonstrated to be an effective photodynamic antimicrobial agent, based on its ability to inactivate or destroy viruses, bacteria, yeasts, and protozoa, as well as this dye having been successfully used in the treatment of psoriasis and different tumors [11–13].

Following on from several investigations carried out on New Fuchsin (**1a** – triarylmethane) and Azure B (**2a** – thiazine) dyes, which have produced guidelines for the development of novel mitochondrial targeted drugs, the aims of the present research were the synthesis of **1b–d** and **2b,c** (Scheme 1) and the evaluation of some photophysical and photochemical properties of importance to biomedical applications, and the determination of photodynamic activity against the LM-2 murine mammary carcinoma cell line using the MTT assay.

Results and discussion

Synthesis and light absorption characteristics of new photosensitizers

The novel brominated dyes were synthesized from **1a** and **2a** with molecular bromine (Br_2) under different reaction conditions giving the derivatives monobromonated (**1b**), dibrominated (**1c**), and tribrominated (**1d**) of New Fuchsin, as well as the derivatives monobromonated (**2b**) and dibrominated (**2c**) of Azure B (Scheme 1). These compounds were *ortho*-brominated derivatives of the activating amine group, due to the *para*-positions being already substituted in the **1a** and **2a** dyes. The **1a** derivatives were easily obtained varying the molar ratios of reagents. Instead, different reaction conditions, such as solvents, reaction time, and temperature had to be evaluated for thiazine products. The Supporting Information S1 summarizes the more relevant synthesis reactions. The Figs. 1 and 2 show the RP-HPLC chromatograms obtained at different molar ratios of dye/Br_2 for **1a** and **2a**, respectively.

The absorption spectra in acetonitrile of **1a–d** (Fig. 3A) displayed a maximum absorption between 540 and 560 nm and a shoulder in the spectral region from 475 to 520 nm. This band has been observed in other extensively studied triarylmethanes such as Crystal Violet. This characteristic spectrum appeared to be composed of two overlapping bands, and different theories have been put forward to account for this [14–16].

The dyes **2a–c** (Fig. 3B) also had a characteristic visible absorption spectrum in the 500–700 nm region, with a maximum between 625–650 nm and a shoulder in the spectral region 570–620 nm.

On comparing the λ_{max} values in the acetonitrile of **1a** ($\lambda_{max} = 546$ nm) and **2a** ($\lambda_{max} = 639$ nm) dyes with those of **1b** ($\lambda_{max} = 554$ nm) and **2b** ($\lambda_{max} = 643$ nm) derivatives, respectively, a bathochromic shift was observed (4–8 nm). The substitution of **1a** and **2a** by two bromine atoms produced the dyes **1c** ($\lambda_{max} = 557$ nm) and **2c** ($\lambda_{max} = 649$ nm), with an increase of 6–11 nm at the maximum wavelength. An additional substitution of **1c** by another bromine atom

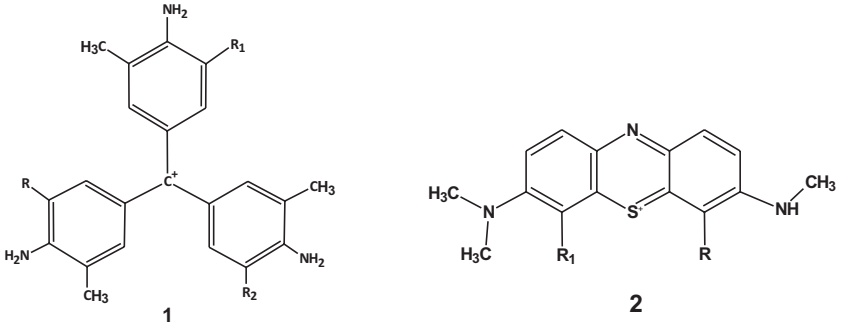

1a	R= R_1= R_2= H	**2a**	R= R_1= H
1b	R= Br R_1= R_2= H	**2b**	R= Br R_1= H
1c	R= R_1= Br R_2= H	**2c**	R= R_1= Br
1d	R= R_1= R_2= Br		

Scheme 1. New derivatives of New Fuchsin (**1a**) and Azure B (**2a**).

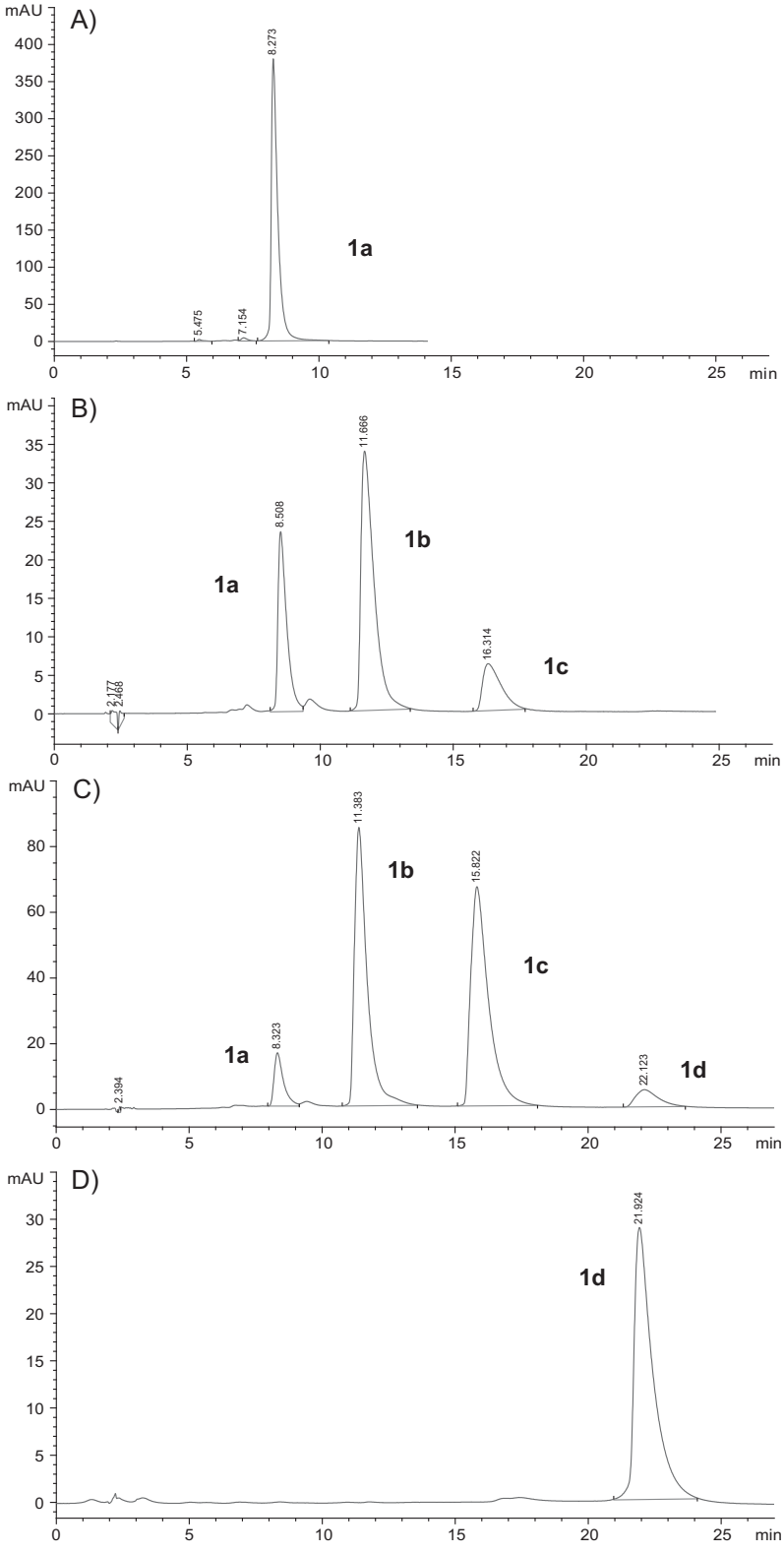

Figure 1. RP-HPLC chromatograms of the reaction **1a**:Br_2 without bromide (A) and at different molar ratios, 1:1 (B), 1:2 (C), and 1:3 (D).

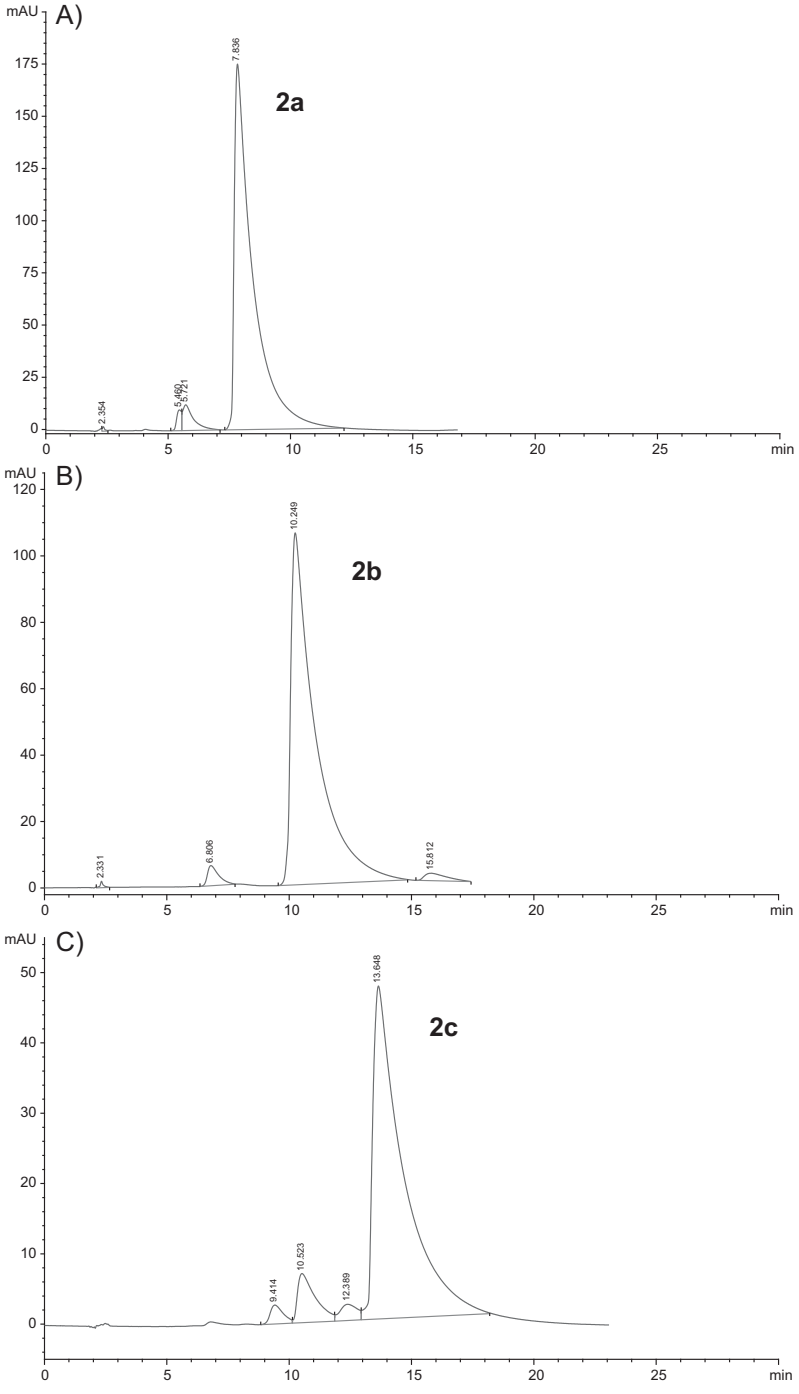

Figure 2. RR-HPLC chromatograms of the reaction **2a**:Br_2 without bromide (A) and at different molar ratios, 1:1 (B) and 1:4 (C).

produced **1d** (λ_{max} = 560 nm), with an increase in λ_{max} of 14 nm compared with **1a**.

Stability test and aggregation effect

Derivatives **1d** and **2b** presented significant changes in the spectral curves in different solvents and as function of dye concentration. For this reason, we evaluated the stability and aggregation effect in physiological conditions of **1d** and **2b** in comparison with their precursors.

The results obtained for dyes **1a**, **2a**, and **2b** demonstrated a high chemical stability at 37°C, pH 7.4 and over 27 h. Moreover, for the new compound **1d**, we observed a

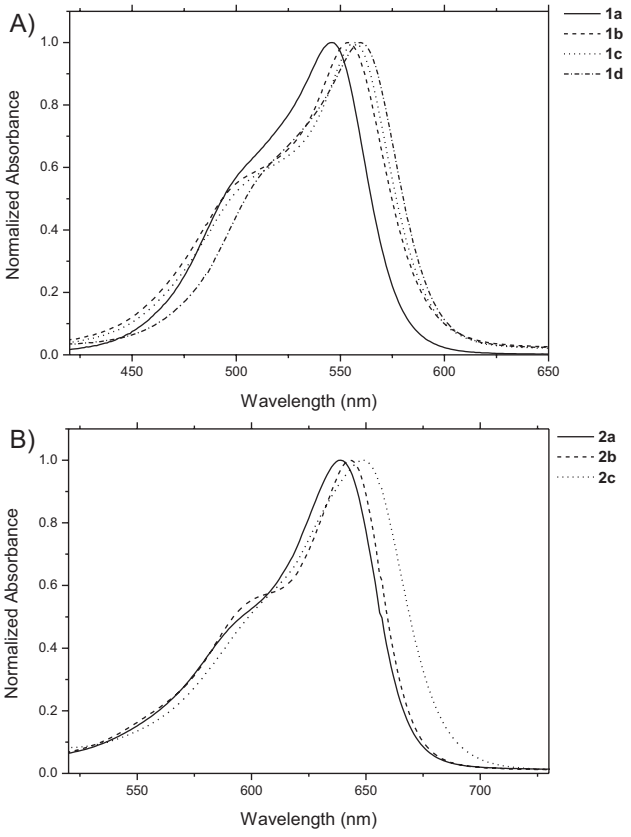

Figure 3. Absorption visible spectra of compounds **1a–d** (A) and **2a–c** (B) in acetonitrile.

decolorized dye solution. This effect was completely reversed by addition of glacial acetic acid, indicating equilibrium between the cationic form and the carbinol base of the dye (data not shown). Some authors have carried out studies concerning the solvent effects in triarylmethane dyes, and have demonstrated that these compounds can exist in the form of colored cations or as colorless carbinol bases [17–20].

Evaluation of the aggregation effect indicated that **1a** and **1d** dyes did not undergo self-association in the experimental conditions assayed. This behavior may be attributed to the addition of polyethylene glycol 400 (PEG 400) (good monomerizing solvent) and the dye concentration ranges studied (10^{-5}–10^{-6} M). Therefore, considering that aggregate formation was inhibited in PEG 400, the behavior of both dyes in buffer pH 7.4/PEG 400 mixture 75:25 v/v as a function of dye concentration indicated that the monomeric form was the predominant species and responsible for the principal band which had an absorption maximum at 555 and 569 nm for **1a** and **1d**, respectively. These results are consistent with those obtained by other authors for Ethyl Violet and Crystal Violet, where these dyes formed aggregates in aqueous solutions at higher concentrations [21].

An interesting observation on the aggregation behavior of **2a** and **2b** dyes in buffer pH 7.4 at different concentrations is shown in Fig. 4. The new dye **2b** (Fig. 4A) showed an absorption band at 650 nm assigned to the monomeric species, due to it being similar to the monomer bands of other thiazine dyes [22, 23]. At the highest dye concentration studied (5.73×10^{-5} M), a shoulder appeared at around 600 nm, which was assigned to the aggregate forms of **2b**. However, the monomeric form was still the predominant band in the spectrum. We compared the absorption spectra of the **2a** and **2b** dyes at 1.2×10^{-5} M (Fig. 4B), and it was clear that the mono-brominated dye showed a higher tendency to aggregate compared with the unsubstituted Azure dye, considering that the relation between the monomer and dimer extinction coefficients being similar for both dyes. The results obtained in this study confirm that thiazine dyes form H-type aggregates in buffer pH 7.4 and **2b** derivative was the compound with higher aggregation tendency. This aggregation effect usually leads to a decrease in the quantum yield in photophysical processes such as singlet oxygen generation, consequently reducing the photodynamic activity of photosensitizers [24–26].

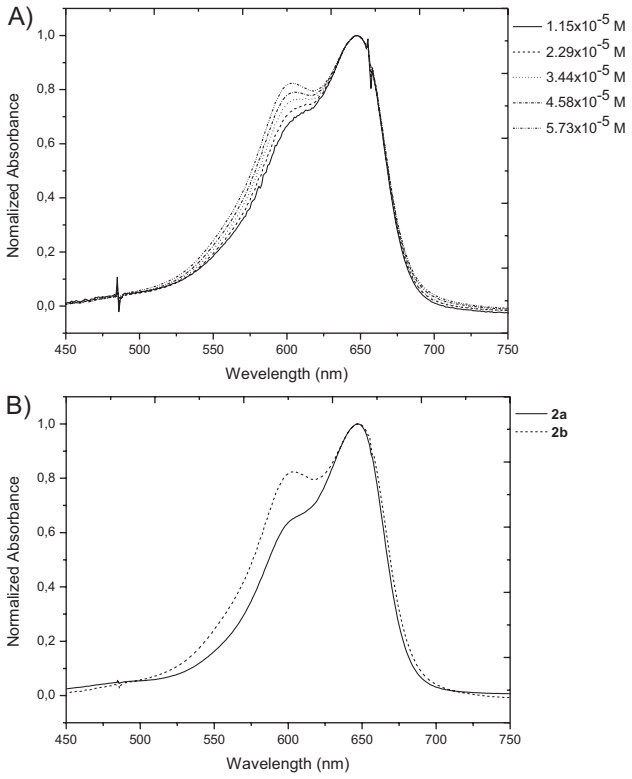

Figure 4. (A) Normalized absorption spectra of **2b** at different concentrations of dye in buffer solution at pH 7.4. (B) Comparison of normalized absorption spectra of compounds **2a** and **2b** at 1.2×10^{-5} M.

Determination of log P_{HPLC}

A dual retention mechanism was observed for **2a–c** dyes (Supporting Information, S2). Previous investigations have reported that a mixed retention mechanism is frequent when protonated bases such as thiazine dyes are involved. The typically U-shaped plots for log k' versus φ (organic modifier) were induced by a rise in retention with an increase in modifier concentration at lower water content (normal-phase behavior, 80–90%), or by an increase in retention time with a decrease in modifier concentration at high water content (reverse-phase behavior, 70–80%) resulting from a mixed retention mechanism between hydrophobic and silanophilic interactions (interaction with residual silanol groups of the stationary phase) [27]. In contrast, a linear relationship between log k' versus φ (70% at 90%) was observed for triarylmethane dyes, **1a–d** (data not shown).

From these plots (log k' *vs.* φ), log k'_w values for all compounds (references and test substances) were calculated and are shown in Table 1. The reverse-phase high performance liquid chromatography (RP-HPLC) correlation between log $P_{O/W}$ and log k'_w for a set of reference compounds was expressed by Eqs. (1) and (2) for triarylmethane and thiazine dyes, respectively. Both equations proved to be excellent fits between the experimental data and log $P_{O/W}$.

$$\log P_{O/W}\,(\mathbf{1a}\text{–}\mathbf{d}) = (1.30 \pm 0.12)\log k'_w - (0.9 \pm 0.4) \quad n = 7;\ r^2 = 0.9527 \tag{1}$$

$$\log P_{O/W}(\mathbf{2a}\text{–}\mathbf{c}) = (1.25 \pm 0.07)\log k'_w - (0.5 \pm 0.2) \quad n = 6;\ r^2 = 0.9824 \tag{2}$$

For all reference compounds and the new brominated dyes, the **1b–d** and **2b,c** log P_{HPLC} values were calculated and are also shown in Table 1.

For this series of compounds, the lipophilicity was dependent on the nature of the substituent in the aromatic phenyl ring, which was increased for compounds with bromine atoms as the substituent. The lipophilicity of the triarylmethane and thiazine dyes were increased in the following order **1a** < **1b** < **1c** < **1d** and **2a** < **2b** < **2c**, respectively. The RP-HPLC method proved to be reliable for the determination of the lipophilicity of triarylmethane and thiazine dyes.

In vitro photodynamic activity

Figure 5A shows histograms of the cell viability (%) of the photosensitizers **1a–d** at 5 μM. Cell survival was not affected by these dyes in the absence of light, but approximately 30% more phototoxicity was observed in LM-2 cells in comparison with dark controls.

Researchers have demonstrated that the substitution by heavy atoms, such as bromine in the chromophoric moiety of triarylmethane photosensitizers, contributes to an increase in the phototoxic properties via the heavy-atom effect [28, 29]. Nevertheless, the compounds under discussion exhibited almost the same phototoxicities as their parent compound **1a**. This may be explained in terms of the neutral carbinol compound that exists in aqueous media in equilibrium with the colored cationic form (photoactive), as we observed for **1d** dye as function of time in dark conditions.

Table 1. Determination of log P_{HPLC} values for new photosensitizers.

Compounds	log $P_{O/W}$[a)]	log k'_w	log P_{HPLC}	
			Triarylmethane dyes[b)]	Thiazine dyes[c)]
References				
Pararosaniline	−0.40	0.83	0.19	–
Azure B (**2a**)	0.70	1.08	–	0.90
Aniline	0.90	1.20	0.69	1.05
New Fuchsin (**1a**)	1.54	1.39	0.94	–
p-Bromoaniline	2.26	1.80	–	1.8
Crystal Violet	3.18	3.47	3.71	–
Bromhexine	4.03	3.62	3.90	4.08
Anthracene	4.54	4.02	4.44	4.58
9-Bromo-phenanthrene	5.45	4.72	4.64	5.45
Test substances				
1b	–	2.43	2.32	–
1c	–	3.15	3.28	–
1d	–	3.51	3.76	–
2b	–	1.45	–	1.36
2c	–	2.11	–	2.19

[a)] Literature data.
[b)] Calculated using Eq. (1).
[c)] Calculated using Eq. (2).

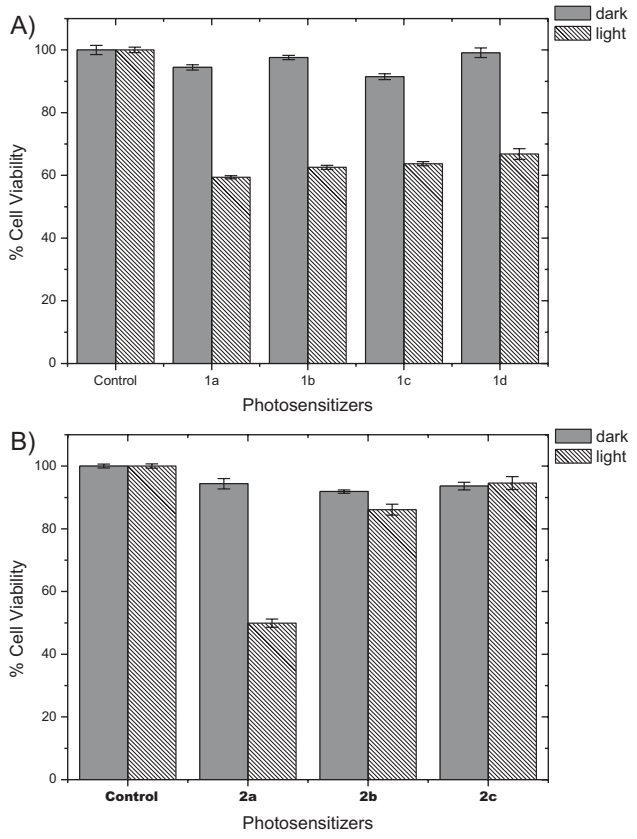

Figure 5. Cytotoxicity and phototoxicity measured in LM-2 murine mammary tumor cells by MTT assay of (A) triarylmethane dyes **1a–d** (0.5 μM) and (B) thiazine dyes **2a,b** (2 μM) and **2c** (0.8 μM).

In vitro cytotoxic activity of thiazine dyes was evaluated in cells pre-incubated with different concentrations of **2a** (0.2–100 μM), **2b** (0.2–2 μM), and **2c** (0.2–2 μM). The survival rates of **2a** and **2b** rose to up to 90% in the absence of light at a concentration of 2 μM. In contrast, **2c** revealed only a moderate cytotoxicity in darkness at the same concentration. In addition, this dye had no detectable toxicity at a concentration of 0.8 μM (data not shown). A potential variation in uptake and intracellular localization may also explain the dark toxicities of the **2c**.

As seen in Fig. 5B, **2a** displayed significant photocytotoxicity and the viability of the LM-2 cells was approximately 50% at 2 μM after PDT treatment. However, no significant lethality was found for cell cultures with the photosensitizers **2b** (2 μM) and **2c** (0.8 μM) after 51 min of light exposure (7 J/cm^2) with a red light-emitting diode (LED) irradiation system.

The relationship between % cell viability and log P_{HPLC} values was also studied, and showed that photodynamic activities against LM-2 cells decreased with increasing log P_{HPLC} values of the different series of brominated dyes, as illustrated in Fig. 6. In contrast with several studies related to different types of photosensitizers, which have indicated that the photosensitizing behavior is governed by the lipophilic character [30], our results demonstrated that the most hydrophilic compound **2a** was the most phototoxic of the series. Although the results obtained in the determination of singlet oxygen showed that the singlet oxygen quantum yields increased with the bromination degree (data not shown), we demonstrated that the photodynamic activity decrease was related to the formation of the colorless carbinol pseudobase for the **1b–d** dyes and an aggregation effect for the **2b** dye.

Appropriate modifications, such as introducing biological conjugates (e.g., antibody conjugate) into the photosensitizer molecule, or by means of encapsulation (e.g., polymeric nanocarriers, polymeric micelles, liposomes, inclusion complexes) of already existing second-generation photosensitizing agents, may lead to creating significantly improved systems on so-called third-generation photosensitizers. Different authors have demonstrated that vehiculization systems can solve problems such as chemical instability, enzymatic decomposition, and photolysis of some photosensitizers, as well as preventing the aggregation of dyes, thus improving the properties of photosensitizers and hence the efficacy and safety of PDT [31–34]. In this way, the new brominated compounds studied could be included into vehiculization systems in order to improve their properties and increase the phototoxicity.

In conclusion, we have described the synthesis and characterization of a novel class of PDT agents. New brominated compounds were prepared by aromatic electrophilic substitution reaction, and the introduction of heavy atoms into the

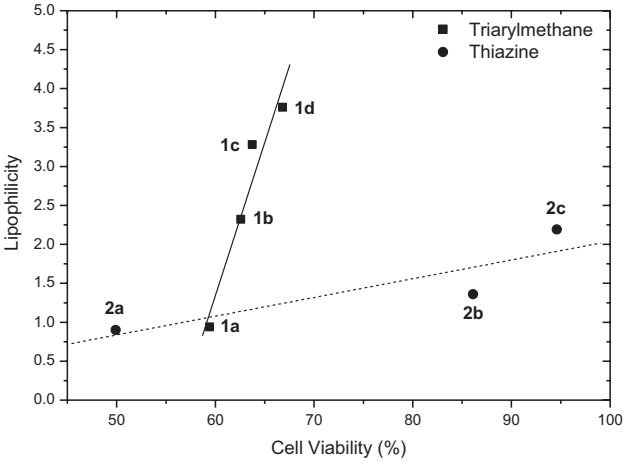

Figure 6. Relationship between photodynamic activity and lipophilicity of triarylmethane and thiazine dyes.

chromophoric system of triarylmethane and thiazine dyes **1a** and **2a** gave rise to a moderate bathochromic shift.

While all brominated dyes showed a log P_{HPLC} in the 0–5 range, considered to be the optimal lipophilicity for mitochondrial photosensitizers, *in vitro* photodynamic activity demonstrated that when the degree of bromination increased, the phototoxicity against the LM-2 mouse mammary tumor cell line stayed unchanged or even decreased. This lower photodynamic efficiency might be attributed to the formation of the colorless carbinol pseudobase for **1b–d** dyes and an aggregation effect for **2b** dye. It is relevant to emphasize that the photodynamic efficacy of each photosensitizer varies according to the target microorganisms and several factors influence the effectiveness of PDT such as chemical structure, physical and chemical properties, and the hydrophilic features of each photosensitizer that allow the free passage across the cellular membrane. The results obtained in the present study should provide encouragement for the development of future studies and highlight the prominent future of the third-generation photosensitizers.

Experimental

General

1a and **2a** (Scheme 1) were purchased at Sigma–Aldrich, St Louis, MO. The dye **1a** was purified by a methodology previously described [35] and **2a** was used as received, both compounds were used at purities >95%. Solvents used for the synthesis, purification, and spectroscopic determinations were of analytical grade, and those used for the chromatographic analysis were of HPLC grade. Reactions were performed using bromine reagent (Carlo Erba, 99.5%).

Thin layer chromatography (TLC) analysis was performed on silica gel 60 F254 (20 × 20 cm^2; 0.25 mm), using the solvent system methylenechloride/ethanol (4:1 v/v) as the eluent for New Fuchsin derivatives, and *n*-buthanol/acetic acid/water (4:1:5 by volume) for the Azure B derivatives [36]. Spectrophotometric determinations were performed on an Agilent 8453 spectrophotometer between 200 and 800 nm. The NMR spectra were obtained on a Bruker Avance II 400 spectrometer equipped with a 5 mm BBI 1H/D-BB ZGRD Z8202/0349 inverse probe and a VTU – Variable Temperature Unit (Bruker BioSpin, Germany), and measurements were obtained in DMSO-d_6/D_2O solution at room temperature. Electrospray ionization mass (ESI–MS) and tandem ESI–MS/MS spectra were recorded on a Varian 1200L triple-quadrupole LC–MS (Varian, USA) spectrometer, with the ESI–MS spectrometer being operated in the positive ion mode. The data acquisition software Varian MS/MS workstation (version 6.6) was used for instrument control, data acquisition, and data handling. The samples were infused directly into the mass spectrometer, and the working concentration was close to 500 ng/mL. Compounds were analyzed on a microQTOF II mass spectrometer (Bruker Daltonics) with an electrospray ionization ion source, operating in the positive mode.

RP-HPLC was carried out using a liquid chromatograph Agilent 1100 Series apparatus equipped with an isocratic pump, a UV–Visible spectrophotometric detector, an autosampler, and a thermostated column compartment. Chromatographic separation was performed with a Supelcosil LC-18, 5 μm; 250 mm × 4.6 mm column (Supelco, Sigma–Aldrich), and detection was carried out at 280 and 550 nm for the New Fuchsin derivatives and at 280 and 640 nm for Azure B derivatives, with the chromatographic system being controlled using the ChemStation (Agilent) software package.

The dye purities were determined by RP-HPLC analysis in all cases, using as the mobile phase a mixture of acetonitrile/ammonium chloride (50 mM; 90:10 v/v) and acetonitrile/triethylamine phosphate (83 mM) (60:40 v/v) for the triarylmethane and thiazine dyes, respectively. The flow rate was 1 mL/min for all determinations.

Bromination of New Fuchsin (1a)

*Monobrominated New Fuchsin (**1b**) and dibrominated New Fuchsin (**1c**)*

To a solution of **1a** (6.06×10^{-5} mol) in 10 mL of glacial acetic acid, bromine solution (1.21×10^{-4} mol, glacial acetic acid) was added at room temperature. The resulting solution containing a mixture of **1b** and **1c** was stirred for 10 min and the solvent was removed under reduced pressure. These compounds were separated by preparative column liquid chromatography (PCLC) using silica gel 60 (70–230 mesh, average pore diameter 60 Å, Sigma Chemical Co, St. Louis, MO) and dichloromethane/ethanol (93:7 v/v and 95:5 v/v) as the eluent to obtain **1b** at a purity of 87% and **1c** at a purity of 93%, respectively.

(**1b**): ^{1}H NMR (DMSO-d_6/D_2O) δ: 1.96 (s, 6H); 2.11 (s, 3H); 6.75 (m, 1H); 6.80 (m, 2H); 6.94 (m, 1H); 7.03 (m, 2H); 7.08 (m, 2H). ^{13}C NMR (DMSO-d_6/D_2O) δ: 17.38; 17.96; 108.66; 114.30; 119.96; 122.58; 127.92; 129.23; 129.77; 129.81; 139.19; 140.59; 144.91; 144.97; 157.08. RP-HPLC t_R: 11.57 ± 0.08 min. TLC R_f: 0.75 ± 0.01. λ_{max} (acetonitrile): 554 nm. ESI–MS *m/z*: 408.2 $[M+H]^+$; 410.2 $[M+H+2]^+$. ESI–MS/MS *m/z* (408.1): 408.1 $[M+H]^+$; 237.2 $[M+H-C_3H_{13}N_3Br]^+$; 148.9 $[M+H-C_{10}H_{17}N_3Br]^+$. ESI–microQTOFF: calculated for $C_{22}H_{23}BrN_3$: 408.1070; found: 408.1086.

(**1c**): ^{1}H NMR (DMSO-d_6/D_2O) δ: 1.97 (s, 3H); 2.06 (s, 6H); 6.74 (m, 2H); 6.81 (m, 1H); 6.94 (m, 2H); 7.05 (m, 1H); 7.07 (m, 1H). ^{13}C NMR (DMSO-d_6/D_2O) δ: 18.12; 19.07; 107.29; 114.30; 120.27; 122.45; 127.79; 128.53; 129.18; 129.44; 141.98; 142.89; 143.14; 145.29; 156.63. RP-HPLC t_R: 15.8 ± 0.1 min. TLC R_f: 0.81 ± 0.02. λ_{max} (acetonitrile): 557 nm. ESI–MS *m/z*: 486.1 $[M+H]^+$; 488.1 $[M+H+2]^+$; 490.1 $[M+H+4]^+$. ESI-MS/MS *m/z* (488.1): 488.1 $[M+H+2]^+$; 392.0 $[M+H+2-H-Br-CH_3]^+$; 301.0 $[M+H+2-H-C_7H_8NBr]^+$; 222.0 $[M+H+2-C_7H_8NBr_2]^+$. ESI-microQTOFF: calculated for $C_{22}H_{22}Br_2N_3$: 486.0180; found: 486.0289.

*Tribrominated New Fuchsin (**1d**)*

A bromine solution (9.09×10^{-5} mol) in glacial acetic acid at room temperature was added dropwise to a solution of **1a** in glacial acetic acid (3.03×10^{-5} mol) while stirring. The resulting solution was stirred for 10 min, and then the solvent was removed by evaporation. The product **1d** was obtained at a purity of 99% without additional purification.

(**1d**): ^{1}H NMR (DMSO-d_6/D_2O) δ: 2.07 (s, 9H); 6.73 (d, 3H, J_{meta} = 1.87); 6.94 (d, 3H, J_{meta} = 1.87). ^{13}C NMR (DMSO-d_6/D_2O) δ: 18.81; 107.47; 122.61; 128.80; 128.88; 140.92; 142.31; 153.21. RP-HPLC t_R: 22.1 ± 0.2 min. TLC R_f: 0.86 ± 0.02. λ_{max} (acetonitrile): 560 nm. ESI–MS *m/z*: 563.9 $[M+H]^+$; 565.9 $[M+H+2]^+$; 567.9 $[M+H+4]^+$; 569.7 $[M+H+6]^+$. ESI–MS/MS *m/z* (567.9): 567.9

$[M+H+4]^+$. ESI-microQTOFF: calculated for $C_{22}H_{21}Br_3N_3$: 563.9286; found: 563.9354.

Bromination of Azure B (2a)

*Monobrominated Azure B (**2b**)*

A solution of bromine (3.7×10^{-5} mol) in methanol was added to a solution of compound **2a** (3.7×10^{-5} mol) in 10 mL of methanol. This mixture was stirred at room temperature for 1 h and the solvent was evaporated under reduced pressure, yielding the new product, **2b**, at a purity of 95%.

(**2b**): ^{1}H NMR (DMSO-d_6/D_2O) δ: 3.14 (s, 3H); 3.43 (s, 6H); 7.43 (d, 1H, $J_{ortho} = 9.22$); 7.60 (d, 1H, $J_{ortho} = 9.11$); 7.75 (s, 1H); 7.97 (d, 1H, $J_{ortho} = 9.11$); 8.04 (d, 1H, $J_{ortho} = 9.22$). ^{13}C NMR (DMSO-d_6/D_2O) δ: 31.02; 41.65; 103.33; 107.94; 116.49; 120.63; 133.08; 135.09; 135.12; 135.96; 138.03; 138.55; 151.66; 154.68. RP-HPLC t_R: 10.2 ± 0.6 min. TLC R_f: 0.45 ± 0.01. λ_{max} (acetonitrile): 643 nm. ESI–MS *m*/*z*: 349.1 $[M+H]^+$; 350.1 $[M+H+2]^+$. ESI–MS/MS *m*/*z* (350.1): 334.0 $[M+H+2-H-CH_3]^+$; 306.0 $[M+H+2-C_2H_6N]^+$. ESI-microQTOFF: calculated for $C_{15}H_{15}BrN_3S$: 348.0170, found: 348.0205.

*Dibrominated Azure B (**2c**)*

A methanolic solution of bromine (1.48×10^{-4} mol) was added to a solution of **2a** (3.7×10^{-5} mol) in 10 mL of methanol. The resulting mixture was stirred at 55–60°C for 30 min. The solvent was removed under vacuum, and the new compound was obtained at a purity of 90%.

(**2c**): ^{1}H NMR (DMSO-d_6/D_2O) δ: 3.22 (s, 3H); 3.44 (s, 6H); 7.59 (d, 1H, $J_{ortho} = 9.60$); 7.62 (d, 1H, $J_{ortho} = 9.39$); 7.92 (d, 1H, $J_{ortho} = 9.39$); 8.00 (d, 1H, $J_{ortho} = 9.60$). ^{13}C NMR (DMSO-d_6/D_2O) δ: 31.49; 44.67; 103.68; 104.12; 119.19; 122.68; 133.78; 135.14; 135.69; 136.03; 136.89; 138.62; 152.55; 155.07. RP-HPLC t_R: 13.8 ± 0.3 min. TLC R_f: 0.51 ± 0.01. λ_{max} (acetonitrile): 649 nm. ESI–MS *m*/*z*: 425.7 $[M+H]^+$; 427.7 $[M+H+2]^+$; 429.7 $[M+H+4]^+$. ESI-MS/MS *m*/*z* (427.7): 401.0 $[M+H+2-H-C_2H_2]^+$; 306.9 $[M+H+2-Br-C_3H_6]^+$. ESI-microQTOFF: calculated for $C_{15}H_{14}Br_2N_3S$: 425.9275, found: 425.9299.

Stability test and aggregation effect

The chemical stability and molecular aggregation phenomena of **1a**, **1d**, **2a**, and **2b** compounds were studied at concentration ranges of 10^{-6}–10^{-5} M in phosphate buffer (KH_2PO_4/NaOH (0.01 M)) adjusted at pH 7.4. PEG 400 at 25% v/v was used as the co-solvent for studying the triarylmethane dyes, due to the poor aqueous solubility of the **1d** dye.

For the stability test, the solutions were placed in a thermostat bath maintained at 37°C over 27 h. At 1 h intervals, samples were withdrawn and analyzed by UV–Vis spectrometry and RP-HPLC by comparing with standard samples.

The aggregation properties were studied as a function of dye concentration at room temperature by absorption UV–Vis spectrometry.

Determination of log P_{HPLC}

The log *P* values were determined for the novel brominated dyes using the RP-HPLC method [37–39]. A set of nine structurally related compounds of known log $P_{O/W}$ values used as references were evaluated to analyze the log $P_{O/W}$–log k'_w relationship. The general procedure consisted of measurement of the retention time (t_R) under isocratic conditions with varying amounts of the organic modifier (φ, methanol) of between 70 and 90% v/v, in 5% increments using as the aqueous phase 40 mM triethylamine phosphate (pH 5.5) [37, 40, 41]. The RP-HPLC was developed using an endcapped non-polar C_{18} stationary reverse phase column at 25°C. The flow rate was 1 mL/min and the injection volume was 50 μL in all cases. A multiwavelength UV–Visible detector was used to monitor signals at 254, 280, 550, and 640 nm, with each chromatographic run being repeated at least twice.

The determination of log $P_{O/W}$ by RP-HPLC is highly dependent on the retention time of solutes and therefore the capacity factor (k'). The k' value for new dyes and the reference compounds were determined at different methanol/water ratios using Eq. (3),

$$k' = \frac{(t_R - t_0)}{t_0} \tag{3}$$

where t_R is the retention time of different compounds, and t_0 is the dead time as measured by using methanol.

A plot of log k' versus φ for each reference compound and test substance was generated, and then the straight line to the 0% modifier was extrapolated to determine log k'_w for each compound as if the eluent were pure water. In this case, k'_w was independent of the organic modifier effect, and the polar- nonpolar partitioning was more similar to the shake measurements and dependent on the solute structure and polar functionalities [42].

Next, a plot of log k'_w of reference compounds versus their known log $P_{O/W}$ values was generated and produced the standard curve given by Eq. (4),

$$\log P_{O/W} = a \log k'_w - b \tag{4}$$

Coefficients *a* and *b*, obtained for each family dye, and the log k'_w values of the brominated dyes **1b–d** and **2b**,**c**, were used to calculate log P_{HPLC} from the standard curve of Eq. (5),

$$\log P_{HPLC} = a \log k'_w - b \tag{5}$$

In all cases, the regression and correlation analyses were performed with OriginPro 8 SR0 (OriginLab Corporation).

In vitro photodynamic activity

Cell culture conditions and photosensitizers

The LM-2 cell line (obtained from Hospital Roffo, Buenos Aires, Argentina) was cultured with Dulbecco's Modified Eagle medium (DMEM) supplemented with 10% heat-inactivated fetal bovine serum, 1% penicillin–streptomycin (100 μg/mL penicillin and 25 μg/mL streptomycin), 50 μg gentamycin, 1% of glutamine (GlutaMAX™ 100x) and 1% of sodium pyruvate 100 mM (Gibco). Cells were kept as a monolayer culture until confluence in culture flasks at 37°C in a humidified incubator with 95% air and 5% CO_2. The cell line was routinely checked for the absence of mycoplasma contamination.

A solution of 20 mM of photosensitizer (purity > 87%) in DMSO was diluted in DMEM containing 1% inactivated fetal bovine serum to a concentration twice as high as the final concentration used in the test.

Photodynamic treatment and cell viability determination

LM-2 cell suspension (1×10^5 cells) was inoculated into each well of a 96-well plate (100 μL/well, Corning, Inc., NY) and incubated

overnight. Then, different concentrations of dyes were added and incubated for 24 h. Subsequently, the plates were irradiated for 60 min using a fluorescent light of 0.362 mW/cm^2 emitted from a TL 20W/03 RS lamp (Phillips, 380–480 nm), which delivered a light dose of 2.08 J/cm^2 for triarylmethane dyes, and a LED array of 2.06 mW/cm^2 (EFOS, Mississauga, Ontario, Canada, 600–650 nm) with 51 min of light exposure (7 J/cm^2) being applied for thiazine dyes.

The light fluence was measured with a radiometer (Laser Mate-Q, Coherent) and cell survival was assessed for untreated (control) and dye-treated cultures. The surviving fraction of cells was evaluated 24 h after treatment by the spectrophotometric method using 3-(4,5-dimethylthiazol-2-yl)-2,5-diphenyltetrazolium bromide (MTT) [43]. This assay is based on the activity of mitochondria dehydrogenases, which can reduce a water-soluble tetrazolium salt to a purple insoluble formazan product. MTT in DMEM was added and the solution was exposed for 3 h to cell cultures at a final concentration of 50 μg/mL. Then, the reduced formazan was extracted with DMSO, and the absorption was measured at 540 nm with a Labsystems Multiskan MS plate reader.

Statistical analyses

All experiments were repeated at least three times independently. Data are shown as the means, and the errors on the graphs represent one standard deviation for at least three independent values. The statistical analyses were performed using Origin Pro 8 SR0 (OriginLab Corporation).

The authors thank Consejo Nacional de Investigaciones Científicas y Técnicas de Argentina (CONICET), Secretaría de Ciencia y Técnica de la Universidad Nacional de Córdoba (SECyT), and Agencia Nacional de Promoción Científica y Tecnológica (ANPCYT) for financial support. The authors would also like to thank Dr. Daniel Wunderlin from Instituto Superior de Recursos Hídricos (IrSRH, Córdoba-Argentina) for developing the mass spectra, Dr. Gloria Bonetto for developing the nuclear magnetic resonance spectra and Dr. Paul Hobson (native speaker) for revision of the manuscript.

References

[1] C. A. Robertson, D. Hawkins Evans, H. Abrahamse, *J. Photochem. Photobiol. B* **2009**, *96*, 1–8.

[2] M. Triesscheijn, P. Baas, J. H. M. Schellens, F. A. Stewart, *Oncologist* **2006**, *11*, 1034–1044.

[3] M. D. Detty, S. L. Gibson, S. J. Wagner, *J. Med. Chem.* **2004**, *47*, 3897–3915.

[4] I. K. Kandela, J. A. Bartlett, G. L. Indig, *Photochem. Photobiol. Sci.* **2002**, *1*, 309–314.

[5] A. S. Don, P. J. H. Hogg, *Trends Mol. Med.* **2004**, *10*, 372–378.

[6] J. Morgan, A. R. Oseroff, *Adv. Drug Deliv. Rev.* **2001**, *49*, 71–86.

[7] J. S. Modica-Napolitano, L. Joyal, G. Ara, A. R. Oseroff, J. R. Aprille, *Cancer Res.* **1990**, *50*, 7876–7881.

[8] E. G. Azenha, A. C. Serra, M. Pineiro, M. M. Pereira, S. J. Seixas de Melo, L. G. Arnaut, S. J. Formosinho, A. M. d'A Rocha Gonsalves, *Chem. Phys.* **2002**, *280*, 177–190.

[9] A. C. Serra, M. Pineiro, A. M. d'A Rocha Gonsalves, M. Abrantes, M. Laranjo, A. C. Santos, M. F. Botelho, *J. Photochem. Photobiol. B* **2008**, *92*, 59–65.

[10] I. K. Kandela, W. Lee, G. L. Indig, *Biotechnol. Histochem.* **2003**, *78*, 157–169.

[11] J. P. Tardivo, A. Del Giglio, C. Santos de Oliveira, D. S. Gabrielli, H. Couto Junqueira, D. Batista Tada, D. Severino, R. Fatima Turchiello, M. S. Baptista, *Photodiag. Photodyn. Ther.* **2005**, *2*, 175–191.

[12] R. F. Donnelly, P. A. McCarron, M. M. Tunney, *Microbiol. Res.* **2008**, *163*, 1–12.

[13] M. Wainwright, *Int. J. Antimicrob. Agents.* **2000**, *16*, 381–394.

[14] S. Lovell, B. J. Marquardt, B. Kahr, *J. Chem. Soc. Perkin. Trans.* **1999**, *2*, 2241–2247.

[15] Y. Maruyama, M. Ishikawa, H. Satozono, *J. Am. Chem. Soc.* **1996**, *118*, 6257–6263.

[16] L. M. Lewis, G. L. Indig, *Dyes Pigments* **2000**, *46*, 145–154.

[17] D. F. Duxbury, *Chem. Rev.* **1993**, *93*, 381–433.

[18] M. Wainwright, S. M. Burrow, S. G. R. Guinot, D. A. Phoenix, J. Waring, *Cytotechnology* **1999**, *29*, 35–43.

[19] H. Ouni, M. Dhahbi, *Sep. Purif. Technol.* **2010**, *72*, 340–346.

[20] A. C. Herath, R. M. G. Rajapaks, A. Wicramasinghe, V. Karunaratne, *Environ. Sci. Technol.* **2009**, *43*, 176–180.

[21] M. L. Lewis, G. L. Indig, *J. Photochem. Photobiol. B* **2002**, *67*, 139–148.

[22] A. Chakraborty, M. Ali, S. K. Saha, *Spectrochim. Acta A* **2010**, *75*, 1577–1583.

[23] K. Patil, R. Pawar, P. Talap, *Chem. Phys.* **2000**, *2*, 4313–4317.

[24] M. Wainwright, A. Shah, K. Meegan, C. Loughran, A. Smith, N. Valli, N. Dempster, *Int. J. Antimicrob. Agents* **2010**, *35*, 405–409.

[25] E. J. Ngen, P. Rajaputra, Y. You, *Bioorg. Med. Chem.* **2009**, *17*, 6631–6640.

[26] L. S. Peloi, R. R. S. Soares, C. E. G. Biondo, V. R. Souza, N. Hioka, E. Kimura, *J. Biosci.* **2008**, *33*, 231–237.

[27] T. Braumann, *J. Chromatogr.* **1986**, *373*, 191–225.

[28] S. H. D. Lacerda, B. Abraham, T. C. Stringfellow, G. L. Indig, *Photochem. Photobiol.* **2005**, *81*, 1430–1438.

[29] J. C. Stockert, A. Juarranz, A. Villanueva, S. Nonell, R. W. Horobin, A. T. Soltermann, E. N. Durantini, V. Rivarola, L. L. Colombo, J. Espada, M. Cañete, *Curr. Top. Pharmacol.* **2004**, *8*, 185–217.

[30] E. G. Friberg, B. Cunderlíková, E. O. Pettersen, J. Moan, *Cancer Lett.* **2003**, *195*, 73–80.

[31] X. He, X. Wu, K. Wang, B. Shi, L. Hai, *Biomaterials* **2009**, *30*, 5601–5609.

[32] H. Zhang, L. Liu, C. Gao, R. Sun, Q. Wang, *Dyes Pigments* **2012**, *94*, 266–270.

[33] C. Lee, Y. W. Sung, J. W. Park, *J. Phys. Chem. B* **1999**, *103*, 893–898.

[34] F. C. Rossetti, L. Biagini Lopes, A. R. Carollo, J. A. Thomazini, A. C. Tedesco, M. V. Lopes Badra Bentley, *J. Controlled Release* **2011**, *155*, 400–408.

[35] M. N. Montes de Oca, I. M. Aiassa, M. N. Urrutia, G. A. Argüello, C. S. Ortiz, *J. Chromatogr. Sci.* **2010**, *48*, 618–623.

[36] J. L. Vennerstrom, M. T. Makler, C. K. Angerhofer, J. A. Williams, *Antimicrob. Agents Chemother.* **1995**, *39*, 2671–2677.

[37] Z. Mrkvickova, P. Kovaríková, S. Balíková, J. Klimes, *J. Pharm. Biomed. Anal.* **2008**, *48*, 310–314.

[38] K. Valko, *J. Chromatogr. A* **2004**, *1037*, 299–310.

[39] G. Cimpan, M. Hadaruga, V. Miclaus, *J. Chromatogr. A* **2000**, *869*, 49–55.

[40] X. Liu, H. Chuman, *J. Med. Invest.* **2005**, *52*, 293–294.

[41] R. Musiol, J. Jampilek, V. Buchta, L. Silva, H. Niedbala, B. Podeszwa, A. Palka, K. Majerz-Maniecka, B. Oleksyn, *J. Bioorg. Med. Chem.* **2006**, *14*, 3592–3598.

[42] S. Griffin, S. Grant Wyllie, J. Markham, *J. Chromatogr. A* **1999**, *864*, 221–228.

[43] T. Mosma, *J. Inmunol. Methods* **1983**, *65*, 55–63.

